Proline residues in transmembrane segment IV are critical for activity, expression and targeting of the Na^+/H^+ exchanger isoform 1

Emily R. SLEPKOV, Signy CHOW, M. Joanne LEMIEUX and Larry FLIEGEL[1]

Membrane Protein Research Group, Department of Biochemistry, Faculty of Medicine, Canadian Institute of Health Research, University of Alberta, 347 Medical Science Building, Edmonton, AB, Canada T6G 2H7

NHE1 (Na^+/H^+ exchanger isoform 1) is a ubiquitously expressed integral membrane protein that regulates intracellular pH in mammalian cells. Proline residues within transmembrane segments have unusual properties, acting as helix breakers and increasing flexibility of membrane segments, since they lack an amide hydrogen. We examined the importance of three conserved proline residues in TM IV (transmembrane segment IV) of NHE1. Pro^{167} and Pro^{168} were mutated to Gly, Ala or Cys, and Pro^{178} was mutated to Ala. Pro^{168} and Pro^{178} mutant proteins were expressed at levels similar to wild-type NHE1 and were targeted to the plasma membrane. However, the mutants P167G ($Pro^{167} \rightarrow$ Gly), P167A and P167C were expressed at lower levels compared with wild-type NHE1, and a significant portion of P167G and P167C were retained intracellularly, possibly indicating induced changes in the structure of TM IV. P167G, P167C, P168A and P168C mutations abolished NHE activity, and P167A and P168G mutations caused markedly decreased activity. In contrast, the activity of the P178A mutant was not significantly different from that of wild-type NHE1. The results indicate that both Pro^{167} and Pro^{168} in TM IV of NHE1 are required for normal NHE activity. In addition, mutation of Pro^{167} affects the expression and membrane targeting of the exchanger. Thus both Pro^{167} and Pro^{168} are strictly required for NHE function and may play critical roles in the structure of TM IV of the NHE.

Key words: cation transport, membrane, Na^+/H^+ exchanger, proline, transmembrane segment IV.

INTRODUCTION

Mammalian NHE (Na^+/H^+ exchanger) isoform 1 is a ubiquitously expressed integral membrane protein that mediates the amiloride-sensitive exchange of one extracellular sodium ion for one intracellular proton [1]. Physiologically, NHE1 functions to protect cells from intracellular acidification [2,3], to stimulate changes in the growth or functional state of cells [2] and to regulate both sodium fluxes and cell volume after osmotic shrinkage [4]. The NHE also plays an important role in the damage that occurs to the human myocardium during ischaemia and reperfusion, and it has been shown that inhibition of the exchanger has beneficial effects on the myocardium under these conditions [5].

The general structure of NHE1 is composed of two domains: an N-terminal membrane domain of approx. 500 amino acids and a C-terminal regulatory domain of approx. 300 amino acids [1,5]. Figure 1(A) depicts a recently determined membrane topology of NHE1 that consists of 12 transmembrane helices with both the N- and C-termini located in the cytosol, as well as a membrane-associated segment and two re-entrant loops [6].

Although NHE1 has been extensively examined, little is known about how this antiporter actually binds and transports Na^+ ions and protons. Several studies have suggested that TM IV (transmembrane segment IV; residues 155–178) is important for the ion transport and inhibitor-binding properties of NHE1 (Figure 1B) [7–9]. TM IV has the sequence ^{155}FLQSDVFFLFLLPPIILDA-GYFLP^{178} in human NHE1. Within this sequence, the underlined residues affect either the Na^+ affinity or inhibitor resistance of human and other mammalian NHEs [7–9]. These results provide a strong case for the importance of TM IV in the ion-binding and transport properties of NHE1.

As shown in the sequence alignment in Figure 2, TM IV contains three highly conserved proline residues. In particular, Pro^{167} and Pro^{168} are preserved across all eight isoforms of the mammalian NHE, although the equivalents of Pro^{168} and Pro^{178} are not conserved in the yeast NHE, NHX-4 [10]. Conservation of Pro^{167} and Pro^{168} in the mammalian NHEs suggests that these proline residues may play an important role in NHE function. Having proline residues in the middle of TM IV could be important for the mechanism of NHE1, since proline residues are considered to be helix breakers. They also lack an amide hydrogen and cause a kink of approx. 26° in the α-helix [11,12]. These characteristics leave the $i-4$ backbone carbonyl without its normal hydrogen bond donor and prevent the formation of the $(i-3)$-carbonyl–$(i+1)$-amide backbone hydrogen bond [11]. In the recent X-ray structure of the glycerol-3-phosphate transporter from *Escherichia coli* [13], two transmembrane helices that contain two sequential proline residues are present. Helix V contains two proline residues and is bent, whereas helix IV contains two proline residues but is straight. Similarly, in the lactose permease of *E. coli*, some kinks in transmembrane segments are at proline residues, although others are at glycine or alanine residues [14]. Therefore it is clear that the effect of proline residues within transmembrane segments varies, that the local environment can moderate them and that kinks in transmembrane segments are not always induced by proline residues. Variability in these effects makes the study of specific proline residues most interesting.

The characteristics of proline residues within transmembrane segments could have several important consequences for TM IV of the NHE. Each proline introduced into an α-helix leaves two free backbone carbonyls, which could directly co-ordinate

Abbreviations used: HA, haemagglutinin; NHE, Na^+/H^+ exchanger; cNHE1, cysteineless NHE1; NHS, *N*-hydroxysuccinimido; TM IV, transmembrane segment IV.

[1] To whom correspondence should be addressed (e-mail lfliegel@ualberta.ca).

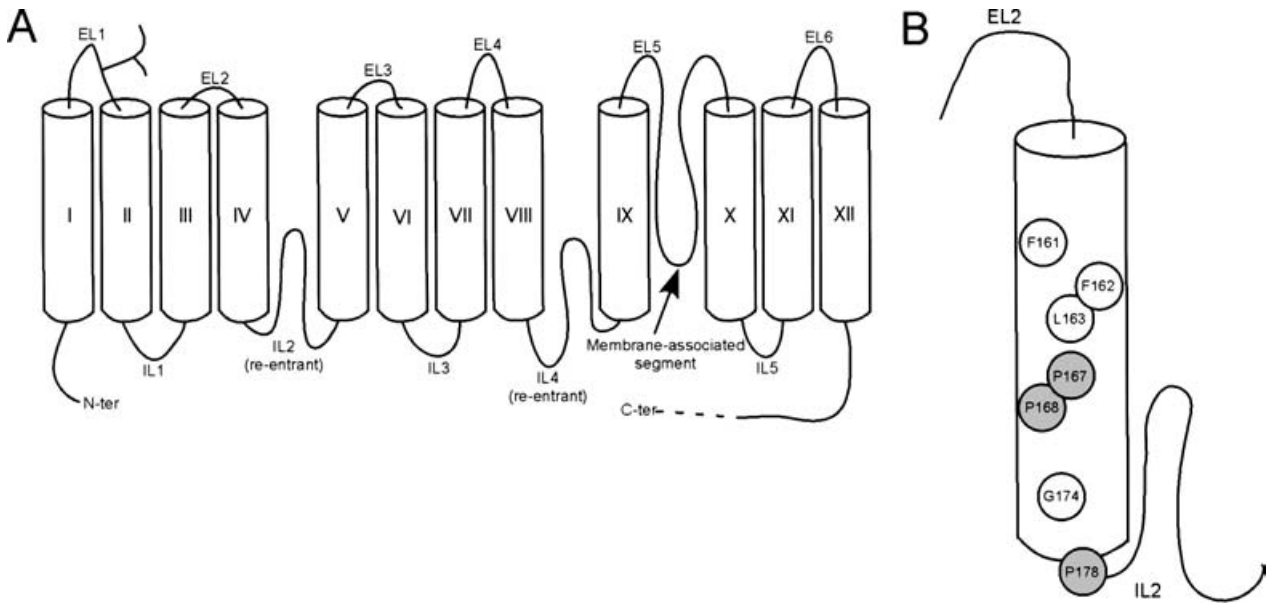

Figure 1 Structural models of NHE1

(**A**) Topological model of NHE1, based on the results of Wakabayashi et al. [6]. The positions of re-entrant intracellular loops and the membrane-associated segment are illustrated. IL, intracellular loop; EL, extracellular loop; ter, terminus. (**B**) Model of TM IV of NHE1 illustrating the positions of the amino acid residues known to be important for NHE1 structure or function. White circles represent the residues that have been suggested previously to be important for NHE1 function. Grey circles represent the conserved proline residues at positions 167, 168 and 178.

```
Human  NHE1 155-FLQSDV FFLFLLPPII LDAGYFLPLR-180
Rat    NHE1 159-FLQSDV FFLFLLPPII LDAGYFLPLR-184
Rabbit NHE1 155-FLQSEV FFLFLLPPII LDAGYFLPLR-180
Human  NHE2  20-AMKTDV FFLYLLPPIV LDAGYFMPTR-45
Human  NHE3 109-TLTPTV FFFYLLPPIV LDAGYFMPNR-134
Rat    NHE4 124-VMDSSI YFLYLLPPIV LESGYFMPTR-149
Human  NHE5 101-QLEPGT FFLFLLPPIV LDSGYFMPSR-126
Human  NHE6 145-TFDPEV FFNILLPPII FYAGYSLKRR-170
Human  NHE7 177-TFDPEV FFNILLPPII FHAGYSLKKR-202
Mouse  NHE8  88-MFRPNM FFLLLLPPII FESGYSLHKG-113
C.e.   NHX4 153-QLDTFM FFMILLPAIV NDAGLSMQKK-178
```

Figure 2 Sequence alignment of NHEs

TM IV of NHE1–8 and NHX4 of *Caenorhabditis elegans* were aligned. Shading indicates identity with the human NHE1 isoform. References are NHE1 [35–37], NHE2 [38], NHE3 [39], NHE4 [36], NHE5 [40], NHE6 [41], NHE7 [42], NHE8 [43] and *C. elegans* (C.e.) [10].

Table 1 Characteristics of glycine, alanine and cysteine residues in comparison with proline residue

The α-helical tendency, probability for the presence of a kink, flexibility introduced into the α-helix and presence of free backbone carbonyl oxygen atoms are indicated for each amino acid.

Amino acid	α-Helical tendency [44]	Kink [11,29]	Flexibility [12,45]	Free carbonyls [12]
Proline	Strong helix breaker	Yes	Yes	Yes
Glycine	Strong helix breaker	Possibly	Yes	No
Alanine	Strong helix former	Possibly	No	No
Cysteine	Helix-indifferent	No	No	No

cations or interact with inhibitors [12]. A kink that is introduced by the proline residues could also create a space to accommodate transported cations or a part of the re-entrant loop, IL2 (intracellular loop 2), which occurs in the NHE [6,8]. The increased flexibility in this transmembrane segment introduced by proline residues could allow for conformational changes that are required for normal exchanger function. Finally, the presence of two proline residues in helix IV may not allow the formation of an α-helix [12].

In the present study, we used site-specific mutagenesis to investigate the functional effects of mutating the conserved proline residues in TM IV. Pro^{178} was mutated to Ala, and Pro^{167} and Pro^{168} were mutated to Gly, Ala or Cys. These amino acids were chosen for the mutations because they differ in their α-helical tendency, backbone flexibility and their ability to cause a kink in the α-helix (Table 1). Mutation of Pro^{178} to Ala had no effect on NHE activity. In all cases, the Pro^{167} and Pro^{168} mutations caused a significant decrease in NHE activity, indicating that these proline residues are critical for normal NHE1 function.

MATERIALS AND METHODS

Plasmids and site-directed mutagenesis

The plasmid pYN4+ contains the cDNA coding for the human NHE1 having an HA (haemagglutinin) tag on the C-terminus of the protein. The plasmid pYN4-C is similar to pYN4+, except that all ten native cysteine residues are mutated to serine residues. Site-directed mutagenesis was performed by amplification with PWO DNA polymerase (Roche Molecular Biochemicals, Mannheim, Germany) using Stratagene Quik Change™ site-directed mutagenesis kit (Stratagene, La Jolla, CA, U.S.A.) according to the manufacturer's instructions. pYN4+ was used as a template for creating the mutants P167G ($Pro^{167} \rightarrow$ Gly), P168G, P167A, P168A and P178A. pYN4-C was used as a template for creating the mutants P167C and P168C. In all cases, the mutations were designed to create a restriction enzyme site that could be used to screen transformants. The accuracy of the mutations was confirmed by sequencing.

Cell culture and stable transfection

AP-1 cells, Chinese-hamster ovary cells that lack endogenous NHE activity, were maintained as described previously [15]. For

transfection, 4×10^5 cells were seeded in a 35 mm Petri dish in 2 ml of growth medium. On the following day, cells were transfected with 4 μg of wild-type or mutagenized plasmid construct using LIPOFECTAMINE™ 2000 Reagent (Invitrogen, Carlsbad, CA, U.S.A.) according to the manufacturer's instructions. The transfected cells were selected using 800 μg/ml geneticin (G418). Cultures were regularly re-established from frozen stocks, and the cells from passage numbers 5–15 were used for experiments.

SDS/PAGE and immunoblotting

Immunoblot analysis was performed on total cell lysates from transfected and untransfected AP-1 cells. Cells were recovered manually from plates in the presence of lysis buffer consisting of 50 mM Tris/HCl (pH 7.4), 150 mM NaCl, 1 % (v/v) Nonidet P40, 0.25 % (w/v) sodium deoxycholate, 0.1 % (v/v) Triton X-100, 1 mM ethylene glycol-bis-(β-aminoethylether)-*N*,*N*,*N*′,*N*′-tetraacetic acid, 0.1 mM benzamidine, 0.1 mM PMSF and 0.1 % (v/v) protease inhibitor cocktail [16]. The protease inhibitor cocktail consisted of 0.5 μg/ml *N*-[*N*-(L-3-*trans*-carboxyoxirane-2-carbonyl)-L-leucyl]agmatine, 0.1 μg/ml aprotinin, 0.5 μg/ml leupeptin, 0.5 μg/ml pepstatin, 50 μg/ml L-1-chloro-3-(4-tosylamido)-7-amino-2-heptane hydrochloride and L-1-chloro-3-(4-tosylamido)-4-phenyl-2-butanone, 0.1 μg/ml (4-amidinophenyl)methanesulphonyl fluoride and 50 μg/ml *N*-(L-rhamnopyranosyloxyhydroxy-phosphinyl)-L-leucyl-L-tryptophan. The cell lysates were centrifuged at 16000 ***g*** for 5 min at 37 °C in an Eppendorf centrifuge 5415 C; for each sample, 100 μg of the total protein was resolved on an SDS/10 % (w/v) polyacrylamide gel. The gel was transferred on to a nitrocellulose membrane and immunostained using 1:2000 dilutions of anti-HA monoclonal antibody (Boehringer Mannheim, Laval, QC, Canada) and peroxidase-conjugated goat anti-mouse antibody (Bio/Can, Mississauga, ON, Canada). Immunoreactive proteins were visualized by enhanced chemiluminescence (Amersham Biosciences) Western blotting and detection system following the manufacturer's instructions. X-ray films were scanned, and densitometric analysis was performed using NIH Image 1.63 software (NIH, Bethesda, MD, U.S.A.).

Cell-surface expression

We measured cell-surface expression essentially by the method described in [17]. Cells grown to approx. 80 % confluence in 60 mm tissue culture dishes were washed with borate buffer (154 mM NaCl/7.2 mM KCl/1.8 mM $CaCl_2$/10 mM boric acid, pH 9.0) at 4 °C and then incubated for 30 min in 3 ml of 0.5 mg/ml sulpho-NHS-SS-biotin (where NHS stands for *N*-hydroxysuccinimido; Pierce Chemical, Rockford, IL, U.S.A.) in borate buffer at 4 °C. The cells were washed three times with cold quenching buffer (192 mM glycine/25 mM Tris, pH 8.3) and then solubilized on ice in 0.5 ml of IP (immunoprecipitation) buffer [1 % (w/v) deoxycholic acid/1 % (w/v) Triton X-100/0.1 % (w/v) SDS/150 mM NaCl/1 mM EDTA/10 mM Tris/HCl, pH 7.5/0.1 mM benzamidine/0.1 mM PMSF/0.1 % (v/v) protease inhibitor cocktail]. After centrifugation at 16000 ***g*** for 20 min to remove the cell debris, half of the supernatant was retained for SDS/PAGE analysis and the remainder was gently rocked overnight at 4 °C with immobilized streptavidin resin [50 μl of 1–3 mg/ml streptavidin settled gel as a 50 % (v/v) slurry in PBS containing 2 mM NaN_3; Pierce Chemical]. The beads were removed by centrifuging at 8000 ***g*** for 2 min and the supernatant was retained. Equivalent amounts of the total and unbound fractions were analysed by SDS/PAGE and Western blotting as described above. The amount of NHE1 on the plasma membrane was calculated by comparing both the 110 and the 95 kDa species of NHE1 in the total and unbound fractions. Results are shown as means ± S.E.M. and statistical significance was determined by Mann–Whitney *U* test.

Immunocytochemistry

To determine the intracellular localization of the NHE, transfected cells expressing wild-type or mutant NHE1 were grown on coverslips to 70–80 % confluence. The coverslips were washed twice with 1 × PBS (pH 7.4; Invitrogen Life Technologies), followed by fixing with methanol for 15 min at −20 °C. The coverslips were then washed twice for 10 min in 1 × PBS. The cells were permeabilized by incubating in TA-PBS (0.1 % BSA and 0.2 % Triton-X-100 in PBS) for 15 min and then washed three times in TA-PBS. The coverslips were blocked in 5 % (v/v) goat serum in TA-PBS for 20 min. After three washes with TA-PBS, coverslips were incubated with mouse monoclonal anti-HA antibody (1:300 in TA-PBS; Boehringer Mannheim) for 1 h at room temperature (21 °C). The cells were washed again three times with TA-PBS, and reacted with Alexa Fluor 488-conjugated goat anti-(mouse IgG) immunoglobulin (1:300 in TA-PBS; Molecular Probes, Eugene, OR, U.S.A.). Finally, the cells were washed three times with PBS, and the coverslips were mounted using Vectasheild (Vector Laboratories, Burlingame, CA, U.S.A.) mounting media with 4′,6-diamidino-2-phenylindole (DAPI). Cells were visualized using a Leica DMIRB fluorescent microscope.

NHE activity

We calculated NHE activity as the initial rate of Na^+-induced recovery of cytosolic pH (intracellular pH) after an acute acid load, as measured fluorimetrically using BCECF [2′,7′-bis-(2-carboxyethyl)-5(6)-carboxyfluorescein; Molecular Probes]. Ammonium chloride was used to transiently induce an acid load, and recovery in the presence of 135 mM NaCl was measured as described previously [15]. There was no difference in the buffering capacity of control versus experimentally transfected cells, as indicated by the degree of acidification induced by ammonium chloride. Measurements of each type of stably transfected cell were repeated on two independently isolated clones of each NHE mutant. Results are shown as means ± S.E.M. and statistical significance was determined using the independent-samples *t*-test. To calculate NHE activity for each amount of protein present on the plasma membrane, NHE activity was normalized to the NHE1 expression levels and cell-surface targeting levels, which were measured as described above.

Protein analysis

TM IV (amino acids 155–177) were analysed using the SAM (Sequence Alignment and Modeling) System [18], which uses the hidden Markov model for homology sequence alignment to assist with secondary-structure prediction using the DSSP program [19].

RESULTS

Expression of mutant NHE1 proteins

The mutations P167G, P168G, P167A, P168A and P178A, introduced into the wild-type NHE, and the mutations P167C and P168C, introduced into a cysteineless version of the NHE, were expressed in the Na^+/H^+ exchange-deficient AP-1 cell line.

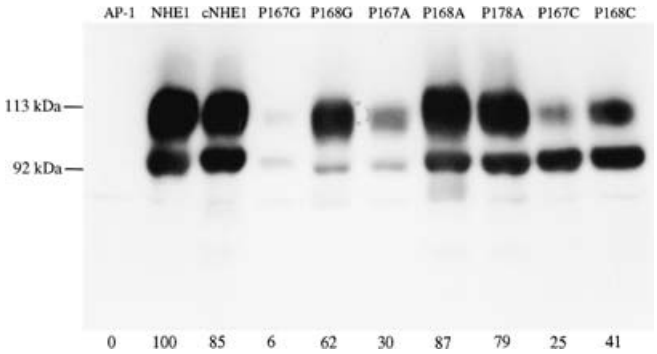

Figure 3 Western-blot analysis of stable transfectants of the NHE

Cells were stably transfected with untransfected AP-1 cells (AP-1), control HA-tagged NHE1 (NHE1), cNHE1 and HA-tagged NHE1 with the mutations P167G, P168G, P167A, P168A, P178A, P167C and P168C, as described in the Materials and methods section; 100 μg of total protein was loaded in each lane. Numbers underneath the lanes indicate the values obtained from densitometric scans of the 110 kDa band relative to wild-type NHE.

Figure 3 shows results of a Western-blot analysis using an anti-HA antibody. A densitometric analysis was performed on this Western blot, and the levels of protein expression relative to that of NHE1 are shown beneath each lane as a percentage of wild-type NHE1 expression. From Figure 3, it can be seen that the mutant and wild-type exchangers displayed the same pattern of immunoreactive bands, with a larger band at approx. 110 kDa, which represents the glycosylated form of the mature NHE, and a smaller band at approx. 95 kDa, which represents an immature form of the exchanger that is not fully glycosylated [20]. The densitometric analysis included only the larger 110 kDa species. The Western blot in Figure 3 demonstrated that the mutant NHEs were all expressed, although P167G, P167A and P167C all have less than one-third of the expression of wild-type NHE1. In addition, the P167G, P167C and P168C mutants had more prominent bands at 95 kDa than at 110 kDa, indicating that a large portion of these mutants may not be glycosylated completely, a phenomenon we had observed previously [15]. Western blotting of AP-1 cells that do not express the NHE demonstrated that the antibody is specific for the expressed, tagged protein.

Subcellular localization of mutant and wild-type NHEs

We have noted previously that mutation of some amino acids of the NHE can cause the protein to be targeted to an intracellular location [15]. We therefore examined the targeting of the NHE by two techniques. First, to obtain a quantitative measurement of the proportion of NHE1 on the plasma membrane, cells were labelled with sulpho-NHS-SS-biotin. Cells were then lysed and solubilized, and the labelled proteins were bound to streptavidin–agarose resin. Equal samples of the total cell lysate and the unbound lysate were run on SDS/polyacrylamide gels, and Western blotting with an anti-HA antibody was used to identify NHE1 protein. Figure 4(A) and Table 2 show examples and summaries of the results respectively.

Figure 4(A) shows representative Western blots used to determine the amount of NHE1 protein present on the plasma membrane (lane T, total amount of NHE1 protein present in each sample; lane I, the fraction of the NHE that did not bind to the streptavidin–agarose beads). Table 2 is a summary of the results in Figure 4(A) and demonstrates that wild-type NHE1, P167A, P168G, P168A, P168C and P178A are predominantly present on the plasma membrane. A moderately less amount of cNHE1

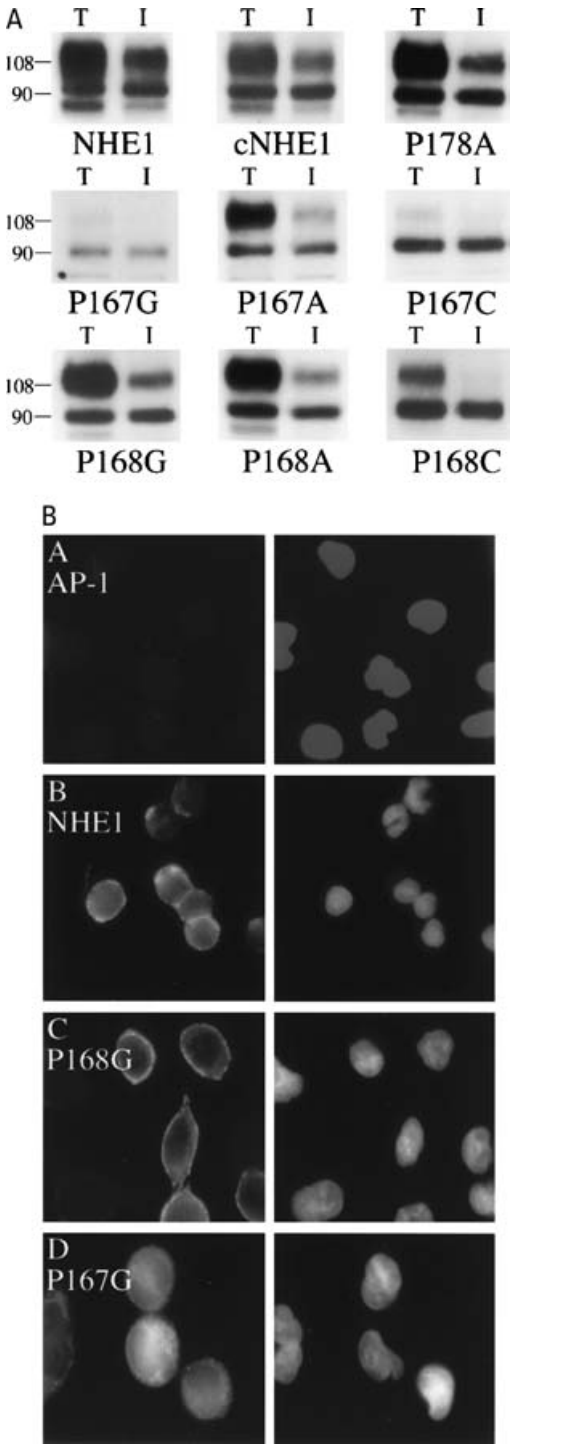

Figure 4 Subcellular trafficking of NHE1

(**A**) Representative Western blots for measuring the subcellular localization of the NHE. Cells were treated with sulpho-NHS-SS-biotin, solubilized, and biotin-labelled proteins were bound to streptavidin–agarose beads as described in the Materials and methods section. A sample of the total cell lysate (T) and an equivalent amount of unbound lysate (I, intracellular) were run on an SDS/polyacrylamide gel. Western blotting with an anti-HA antibody was used to identify the NHE1 protein. NHE1, wild-type NHE1. (**B**) Immunocytochemical localization of the NHE protein, demonstrating plasma-membrane and intracellular localization. Transfected and untransfected cells were prepared for immunocytochemical analysis using anti-HA antibody, as described in the Materials and methods section. A, untransfected AP-1 cells; B, wild-type NHE1; C, P168G; and D, P167G. Left panel: immunofluorescent staining using an anti-HA antibody. Right panel: nuclear localization by 4′,6-diamidino-2-phenylindole staining.

Table 2 Summary of the subcellular localization of wild-type NHE1, cNHE1 and mutant NHEs (P167G, P168G, P167A, P168A, P178A, P167C and P168C)

Localization of NHE1 and mutants was determined as described in the Materials and methods section. The percentage of the total NHE1 protein found within the plasma membrane is indicated. Results are the means ± S.E.M. for at least three determinations. NHE1, wild-type NHE1.

Cell line	Plasma membrane (% of the total)
NHE1	62.5 ± 3.9
P167A	66.7 ± 3.2
P167G	26.8 ± 11.6*
P168A	64.8 ± 3.7
P168G	57.1 ± 5.4
P178A	54.4 ± 2.6
cNHE1	40.0 ± 3.3*
P167C	23.4 ± 7.8*
P168C	51.9 ± 1.9

* Mutants that have significantly less plasma-membrane localization compared with NHE1 (Mann–Whitney U test, $P < 0.05$).

Table 3 Summary of rate of recovery from an acid load by untransfected AP-1 cells and AP-1 cells stably transfected with wild-type NHE1, cNHE1 and mutant NHEs (P167G, P168G, P167A, P168A, P178A, P167C and P168C)

NHE activity was measured after transient induction with an acid load as described in the Materials and methods section. The activity of the cells stably transfected with NHE1 was 3.3 pH units/min, and this value was set to 100 %. Results are the means ± S.E.M. for at least 11 determinations from two independently prepared stable cell lines. The 95 % confidence limits are shown in brackets. Corrected activity indicates activity normalized for the amount of protein expressed and targeted to the plasma membrane after subtraction of the background activity.

Cell line	Activity (% of control)	Corrected activity
AP-1	5.0 ± 0.4 (4.2–5.8)	0
NHE1	100.0 ± 7.7 (84.2–115.8)	100 ± 7.7 (84.2–115.8)
cNHE1	97.7 ± 5.4 (85.7–109.7)	179 ± 9.9 (156.9–201.1)
P167A	9.0 ± 0.6*† (7.8–10.2)	18 ± 1.2*† (15.6–20.4)
P167C	3.2 ± 0.3* (2.6–3.8)	0*
P167G	3.9 ± 1.0* (1.9–6.1)	0*
P168A	6.8 ± 1.1* (4.6–9.0)	2 ± 0.3* (1.4–2.6)
P168C	4.5 ± 0.5* (3.5–5.5)	0*
P168G	9.5 ± 1.1*† (7.2–11.8)	8 ± 1.0*† (5.9–10.1)
P178A	79.5 ± 4.0† (71.2–87.8)	114 ± 5.7† (102.1–125.9)

* Mutants with activity significantly less than wild-type NHE1 activity (independent-samples t-test, $P < 0.01$).

† Mutants that retained significantly more activity when compared with untransfected AP-1 cells (independent-samples t-test, $P < 0.01$).

(cysteineless NHE1) was present on the plasma membrane in comparison with the wild-type, and both P167G and P167C mutants were mostly present within the cell.

To illustrate the targeting of NHE1 within the cell, immunocytochemistry was used. Figure 4(B) illustrates some examples of immunocytochemical localization of the NHE, showing both plasma-membrane and intracellular localization. Control, untransfected AP-1 cells showed no plasma-membrane localization. Cells transfected with wild-type NHE (NHE1) or the P168G mutant showed strong plasma-membrane localization. In contrast, cells transfected with the mutant P167G showed an intracellular localization of the NHE.

Effect of mutations on NHE activity

Table 3 shows the activity of the mutant and wild-type NHEs as determined by monitoring the initial rate of recovery in response to an NH_4Cl-induced acid load, and Figure 5 shows examples of results obtained for some of the mutants. When AP-1 cells transfected with NHE1 were exposed to Na^+ after being acidified, there was an immediate and rapid increase in intracellular pH at the rate of 3.30 pH units/min. Both the cNHE1 and P178A mutants displayed essentially the same rate of recovery as wild-type NHE1. In contrast, the mutants P167G, P168A, P167C and P168C had essentially the same rate of recovery as untransfected AP-1 cells (> 2 % of control values). Although the P167A and P168G mutants also had severely decreased rates of recovery, these mutants did retain significantly more activity compared with untransfected AP-1 cells ($P < 0.01$). P167A protein was not expressed to as high a level as wild-type NHE; hence, correction for the level of protein and intracellular targeting (Table 3) showed that it possessed 18 % of wild-type activity. For P167G, P168A, P167C, P168C and P168G, the decreased activity of the mutant proteins cannot be accounted for by the decreased expression or intracellular targeting of the mutant exchangers.

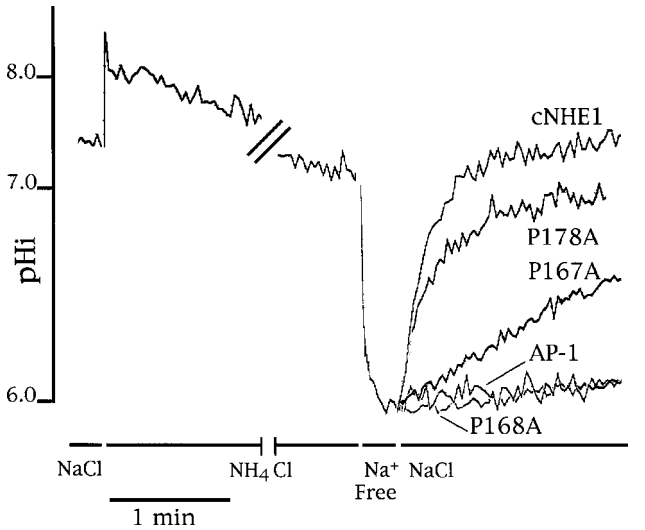

Figure 5 Rate of recovery from an acid load by AP-1 cells containing NHE mutants

Cells were prepared by stable transfection with mutant NHE DNA. Recovery from an NH_4Cl-induced acid load was measured as described in the Materials and methods section. One example of the entire procedure is shown along with typical rates of recovery for cells lines, including untransfected AP-1 cells and AP-1 cells stably expressing cNHE1 or the mutants P167A, P168A and P178A. Results are typical of 10–20 determinations from two independently prepared stable cell lines.

Analysis of TM IV

Table 4 is a secondary-structure prediction of amino acids 155–177 of TM IV. Native TM IV with two proline residues is predicted to be in an extended-strand conformation with little helical structure. In the region of the proline residues themselves, a coil is predicted instead of an α-helix. After substitution of either Pro^{167} or Pro^{168} with alanine, there was a large change in the predicted structure of the TM IV. Substitution of either of the proline residues with an alanine resulted in a helical prediction for most of the TM segment. Substitution of both native proline residues with alanine resulted in the prediction of a helical structure with a higher degree of confidence. It is recognized that the effect of proline residues on the conformation of a protein will vary depending on the local environment of the transmembrane segment [13].

Table 4 Secondary-structure analysis of TM IV of the NHE

Amino acids 155–177 were analysed by sequence alignment and modelling system using the hidden Markov model for homology sequence alignment to assist in secondary-structure prediction using the DSSP program [18,19]. The proline residues of interest are shown in bold. Pss, secondary-structure prediction of either coil (C), extended strand (E), α-helix (H) or hydrogen-bonded turn (T); Prb, probability of the prediction.

Amino acid no.	Amino acid	Native sequence		Both Pro residues substituted with Ala		Pro^{167} substituted with Ala		Pro^{168} substituted with Ala	
		Pss	Prb	Pss	Prb	Pss	Prb	Pss	Prb
155	F	C	0.92	C	0.92	C	0.997	C	0.996
156	L	C	0.79	C	0.77	C	0.767	C	0.761
157	Q	C	0.67	C	0.55	C	0.381	C	0.415
158	S	C	0.62	H	0.61	H	0.513	H	0.423
159	D	C	0.55	H	0.75	H	0.621	H	0.537
160	V	E	0.35	H	0.86	H	0.730	H	0.652
161	F	E	0.49	H	0.89	H	0.745	H	0.686
162	F	E	0.53	H	0.93	H	0.768	H	0.719
163	L	E	0.52	H	0.94	H	0.756	H	0.671
164	F	E	0.50	H	0.93	H	0.678	H	0.609
165	L	E	0.42	H	0.93	H	0.584	H	0.569
166	L	C	0.63	H	0.94	H	0.492	H	0.467
167	**P**	C	0.71	H	0.94	H	0.484	H	0.655
168	**P**	C	0.53	H	0.92	H	0.516	H	0.637
169	I	H	0.34	H	0.89	H	0.532	H	0.619
170	I	E	0.45	H	0.84	H	0.467	H	0.547
171	L	C	0.35	H	0.79	H	0.411	H	0.491
172	D	C	0.51	H	0.64	H	0.353	H	0.425
173	A	C	0.60	H	0.51	T	0.286	H	0.316
174	G	C	0.69	C	0.66	T	0.353	T	0.356
175	Y	C	0.66	C	0.67	C	0.362	C	0.349
176	F	C	0.74	C	0.75	C	0.701	C	0.694
177	L	C	0.98	C	0.98	C	0.998	C	0.998

DISCUSSION

TM IV of the NHE contains several residues that are important for ion transport and inhibitor binding [7–9]. Although their effects on membrane protein structure can vary [13], proline residues are required for expression and targeting to the plasma membrane in a number of membrane proteins [21–23]. We examined the importance of the three conserved proline residues Pro^{167}, Pro^{168} and Pro^{178} in TM IV. Our results demonstrated that both Pro^{167} and Pro^{168} were critical for proper NHE activity, whereas Pro^{178} was not. In addition, Pro^{167} and Pro^{168} had varied effects on NHE1 targeting and expression. Whereas Pro^{167} was critical for expression and membrane targeting of NHE1, mutation of Pro^{168} did not influence targeting and had lesser effects on expression levels. For Pro^{167}, a large fraction of both P167G and P167C was retained within the cell and all mutations of Pro^{167} had significantly decreased levels of NHE1 protein expression. In addition, the P167G and P167C mutants had no NHE activity remaining and the P167A mutant retained only 18 % of the activity of the wild-type. For Pro^{168}, all of the mutants had either severely impaired or no NHE activity. However, in contrast with Pro^{167}, Pro^{168} mutant expression levels were only moderately decreased and targeting was not significantly impaired. Thus both Pro^{167} and Pro^{168} were critical for NHE activity. It is worth noting that, even though both proline residues are conserved in the mammalian NHE isoforms, Pro^{168} is not conserved in the yeast NHE, NHX-4 [10]. Our finding that mutation of Pro^{168} has lesser effects on NHE1 is consistent with this observation.

Why Pro^{167} affects the targeting and expression levels of NHE1 is not clear at present. It may be that Pro^{167} specifically affects TM IV conformation, causing a specific alteration in structure that does not occur at amino acids 168 and 178. The decreased expression levels of Pro^{167} could be accounted for by protein quality-control systems, consisting of chaperones and proteases [24–26] that degrade mutated proteins, affecting folding and targeting. Pro^{167} could thus be important for the conformation of helix IV or for helix–helix interactions that affect conformation. This suggestion is similar to the case of bacteriorhodopsin, where Pro^{50} and Pro^{91} contribute to the folding of the protein [27].

Several results suggested that the functional consequence of mutating Pro^{167} and Pro^{168} were probably due to specific effects on TM IV of NHE1 rather than a general effect that occurs in all proteins with mutation of proline residues. First, we found that the effects of mutating Pro^{167} and Pro^{168} are specific to these specific transmembrane proline residues, since Pro^{178} could be mutated to alanine without affecting NHE activity. Secondly, it has shown previously that the mutation P239A in TM VI of NHE1 also had no effect on NHE activity [15]. Finally, proline residues in transmembrane helices of other membrane proteins can be mutated and do not always affect protein function [22,28,29].

Our findings regarding important functional roles for Pro^{167} and Pro^{168} match the results of previous studies on other integral-membrane proteins. Mutation of any of the proline residues in the transmembrane helices of the Ca^{2+}-ATPase of the sarcoplasmic reticulum decreased the activity of the enzyme [30]. Similarly, in the human glucose transporter GLUT1, the mutation of proline residues in TM X to either Glu or Ile caused a significant decrease in 2-deoxy-D-glucose uptake [23,31]. In addition, several proline residues were required for the normal function of the *lac* permease in *E. coli* [28,32].

There are several mechanisms by which alterations in Pro^{167} and Pro^{168} could affect the NHE conformation. Proline residues allow free backbone carbonyls at positions 3 and 4 of α-helices, and their presence causes a steric clash between the proline ring and the backbone carbonyl group at position 4 [33,34]. This induces flexibility in this region and can cause kinks in TM helices. A

recent analysis of the distribution of proline residues within TM helices of proteins with known structure revealed that proline residues occur with a relatively high frequency in the middle of TM helices. This induces a hinge region before the proline residue [34]. In this analysis of the effects of proline residues within TM helices [34], the effect of adjacent proline residues was not examined, but these would presumably cause even greater alterations in the structure of TM segments. Changes to this type of unusual double-proline structure are probably capable of influencing the structure and activity of the NHE. Our prediction of the structure of TM IV (Table 4) agrees with the suggestion that Pro^{167} and Pro^{168} can significantly affect the structure of this segment. Even substitution of alanine for either Pro^{167} or Pro^{168} resulted in marked changes in the prediction of the structure of TM IV. This result agrees with our experiments showing that other residues were unable to substitute effectively for a proline residue regardless of their character. Glycine, alanine and cysteine residues vary in their α-helical propensity and flexibility. However, a glycine or alanine or cysteine residue could not effectively substitute for the proline residue at either of the positions. Thus the tendency to either be flexible or break an α-helix was not the critical determinant of NHE function. An alanine residue was capable of substituting for Pro^{167} to a small degree. It is not clear why an alanine residue allowed partial activity of the NHE. It may be that packing constraints allowed the retention of an appropriate conformation only in the presence of the alanine residue. Further studies on the conformation of this transmembrane segment are necessary to understand how these small mutations could have such major effects on the expression and targeting of the NHE.

This work was supported by a grant to L. F. from CIHR (Canadian Institute of Health Research). E. R. S. is supported by personal awards from the Heart and Stroke Foundation of Canada and Alberta Heritage Foundation for Medical Research. M. J. L. is supported by the CIHR Strategic Training Initiative in Membrane Proteins and Cardiovascular Disease. L. F. is supported by an Alberta Heritage Foundation for Medical Research Scientist Award. We are grateful to Dr D. DiBattista (Brock University, St. Catharines, ON, Canada) for his assistance with the statistical analysis.

REFERENCES

1 Orlowski, J. and Grinstein, S. (1997) Na^+/H^+ exchangers of mammalian cells. J. Biol. Chem. **272**, 22373–22376

2 Grinstein, S., Rotin, D. and Mason, M. J. (1989) Na^+/H^+ exchange and growth factor-induced cytosolic pH changes. Role in cellular proliferation. Biochim. Biophys. Acta **988**, 73–97

3 Pouyssegur, J., Sardet, C., Franchi, A., L'Allemain, G. and Paris, S. (1984) A specific mutation abolishing Na^+/H^+ antiport activity in hamster fibroblasts precludes growth at neutral and acidic pH. Proc. Natl. Acad. Sci. U.S.A. **81**, 4833–4837

4 Shrode, L. D., Cabado, A. G., Goss, G. G. and Grinstein, S. (1996) Role of the Na^+/H^+ antiporter isoforms in cell volume regulation. In The Na^+/H^+ Exchanger (Fliegel, L., ed.), pp. 101–122, R.G. Landes, Austin, TX

5 Fliegel, L. (2001) Regulation of myocardial Na^+/H^+ exchanger activity. Basic Res. Cardiol. **96**, 301–305

6 Wakabayashi, S., Pang, T., Su, X. and Shigekawa, M. (2000) A novel topology model of the human Na^+/H^+ exchanger isoform 1. J. Biol. Chem. **275**, 7942–7949

7 Counillon, L., Franchi, A. and Pouyssegur, J. (1993) A point mutation of the Na^+/H^+ exchanger gene (NHE1) and amplification of the mutated allele confer amiloride resistance upon chronic acidosis. Proc. Natl. Acad. Sci. U.S.A. **90**, 4508–4512

8 Counillon, L., Noel, J., Reithmeier, R. A. and Pouyssegur, J. (1997) Random mutagenesis reveals a novel site involved in inhibitor interaction within the fourth transmembrane segment of the Na^+/H^+ exchanger-1. Biochemistry **36**, 2951–2959

9 Touret, N., Poujeol, P. and Counillon, L. (2001) Second-site revertants of a low-sodium-affinity mutant of the Na^+/H^+ exchanger reveal the participation of TM4 into a highly constrained sodium-binding site. Biochemistry **40**, 5095–5101

10 Nehrke, K. and Melvin, J. E. (2002) The NHX family of Na^+–H^+ exchangers in *Caenorhabditis elegans*. J. Biol. Chem. **277**, 29036–29044

11 Barlow, D. J. and Thornton, J. M. (1988) Helix geometry in proteins. J. Mol. Biol. **201**, 601–619

12 Sansom, M. S. (1992) Proline residues in transmembrane helices of channel and transport proteins: a molecular modelling study. Protein Eng. **5**, 53–60

13 Huang, Y., Lemieux, M. J., Song, J., Auer, M. and Wang, D. N. (2003) Structure and mechanism of the glycerol-3-phosphate transporter from *Escherichia coli*. Science **301**, 616–620

14 Abramson, J., Smirnova, I., Kasho, V., Verner, G., Kaback, H. R. and Iwata, S. (2003) Structure and mechanism of the lactose permease of *Escherichia coli*. Science **301**, 610–615

15 Murtazina, R., Booth, B. J., Bullis, B. L., Singh, D. N. and Fliegel, L. (2001) Functional analysis of polar amino-acid residues in membrane associated regions of the NHE1 isoform of the mammalian Na^+/H^+ exchanger. Eur. J. Biochem. **268**, 4674–4685

16 Michalak, M., Fliegel, L. and Wlasichuk, K. (1990) Isolation and characterization of calcium binding glycoproteins of cardiac sarcolemmal vesicles. J. Biol. Chem. **265**, 5869–5874

17 Sterling, D. and Casey, J. R. (1999) Transport activity of AE3 chloride/bicarbonate anion-exchange proteins and their regulation by intracellular pH. Biochem. J. **344**, 221–229

18 Karplus, K., Barrett, C. and Hughey, R. (1998) Hidden Markov models for detecting remote protein homologies. Bioinformatics **14**, 846–856

19 Kabsch, W. and Sander, C. (1983) Dictionary of protein secondary structure: pattern recognition of hydrogen-bonded and geometrical features. Biopolymers **22**, 2577–2637

20 Counillon, L., Pouyssegur, J. and Reithmeier, R. A. (1994) The Na^+/H^+ exchanger NHE-1 possesses N- and O-linked glycosylation restricted to the first N-terminal extracellular domain. Biochemistry **33**, 10463–10469

21 Lin, Z., Itokawa, M. and Uhl, G. R. (2000) Dopamine transporter proline mutations influence dopamine uptake, cocaine analog recognition, and expression. FASEB J. **14**, 715–728

22 Hong, S., Ryu, K. S., Oh, M. S., Ji, I. and Ji, T. H. (1997) Roles of transmembrane prolines and proline-induced kinks of the lutropin/choriogonadotropin receptor. J. Biol. Chem. **272**, 4166–4171

23 Wellner, M., Monden, I., Mueckler, M. M. and Keller, K. (1995) Functional consequences of proline mutations in the putative transmembrane segments 6 and 10 of the glucose transporter GLUT1. Eur. J. Biochem. **227**, 454–458

24 Seibert, F. S., Loo, T. W., Clarke, D. M. and Riordan, J. R. (1997) Cystic fibrosis: channel, catalytic, and folding properties of the CFTR protein. J. Bioenerg. Biomembr. **29**, 429–442

25 Bross, P., Corydon, T. J., Andresen, B. S., Jorgensen, M. M., Bolund, L. and Gregersen, N. (1999) Protein misfolding and degradation in genetic diseases. Hum. Mutat. **14**, 186–198

26 Gregersen, N., Bross, P., Andrese, B. S., Pedersen, C. B., Corydon, T. J. and Bolund, L. (2001) The role of chaperone-assisted folding and quality control in inborn errors of metabolism: protein folding disorders. J. Inherit. Metab. Dis. **24**, 189–212

27 Lu, H., Marti, T. and Booth, P. J. (2001) Proline residues in transmembrane α helices affect the folding of bacteriorhodopsin. J. Mol. Biol. **308**, 437–446

28 Consler, T. G., Tsolas, O. and Kaback, H. R. (1991) Role of proline residues in the structure and function of a membrane transport protein. Biochemistry **30**, 1291–1298

29 Shelden, M. C., Loughlin, P., Tierney, M. L. and Howitt, S. M. (2001) Proline residues in two tightly coupled helices of the sulphate transporter, SHST1, are important for sulphate transport. Biochem. J. **356**, 589–594

30 Vilsen, B., Andersen, J. P., Clarke, D. M. and MacLennan, D. H. (1989) Functional consequences of proline mutations in the cytoplasmic and transmembrane sectors of the Ca^{2+}-ATPase of sarcoplasmic reticulum. J. Biol. Chem. **264**, 21024–21030

31 Tamori, Y., Hashiramoto, M., Clark, A. E., Mori, H., Muraoka, A., Kadowaki, T., Holman, G. D. and Kasuga, M. (1994) Substitution at Pro^{385} of GLUT1 perturbs the glucose transport function by reducing conformational flexibility. J. Biol. Chem. **269**, 2982–2986

32 Lolkema, J. S., Puttner, I. B. and Kaback, H. R. (1988) Site-directed mutagenesis of Pro^{327} in the lac permease of *Escherichia coli*. Biochemistry **27**, 8307–8310

33 Brandl, C. J. and Deber, C. M. (1986) Hypothesis about the function of membrane-buried proline residues in transport proteins. Proc. Natl. Acad. Sci. U.S.A. **83**, 917–921

34 Cordes, F. S., Bright, J. N. and Sansom, M. S. (2002) Proline-induced distortions of transmembrane helices. J. Mol. Biol. **323**, 951–960

35 Sardet, C., Franchi, A. and Pouysségur, J. (1989) Molecular cloning, primary structure, and expression of the human growth factor-activatable Na^+/H^+ antiporter. Cell (Cambridge, Mass.) **56**, 271–280

36 Orlowski, J., Kandasamy, R. A. and Shull, G. E. (1992) Molecular cloning of putative members of the Na/H exchanger gene family. J. Biol. Chem. **267**, 9331–9339

37 Tse, C. M., Ma, A. I., Yang, V. W., Watson, A. J., Levine, S., Montrose, M. H., Potter, J., Sardet, C., Pouyssegur, J. and Donowitz, M. (1991) Molecular cloning and expression of a cDNA encoding the rabbit ileal villus cell basolateral membrane Na^+/H^+ exchanger. EMBO J. **10**, 1957–1967

38 Ghishan, F. H., Knobel, S. M. and Summar, M. (1995) Molecular cloning, sequencing, chromosomal localization, and tissue distribution of the human Na^+/H^+ exchanger (SLC9A2). Genomics **30**, 25–30

39 Brant, S. R., Yun, C. H. C., Donowitz, M. and Tse, C. M. (1995) Cloning, tissue distribution, and functional analysis of the human Na^+/H^+ exchanger isoform, NHE3. Am. J. Physiol. **269**, C198–C206

40 Baird, N. R., Orlowski, J., Szabo, E. Z., Zaun, H. C., Schultheis, P. J., Menon, A. G. and Shull, G. E. (1999) Molecular cloning, genomic organization, and functional expression of Na^+/H^+ exchanger isoform 5 (NHE5) from human brain. J. Biol. Chem. **274**, 4377–4382

41 Numata, M., Petrecca, K., Lake, N. and Orlowski, J. (1998) Identification of a mitochondrial Na^+/H^+ exchanger. J. Biol. Chem. **273**, 6951–6959

42 Numata, M. and Orlowski, J. (2001) Molecular cloning and characterization of a novel (Na^+, K^+)/H^+ exchanger localized to the *trans*-Golgi network. J. Biol. Chem. **276**, 17387–17394

43 Goyal, S., Vanden Heuvel, G. and Aronson, P. S. (2003) Renal expression of novel Na^+/H^+ exchanger isoform NHE8. Am. J. Physiol. Renal Physiol. **284**, F467–F473

44 Chou, P. Y. and Fasman, G. D. (1978) Prediction of the secondary structure of proteins from their amino acid sequence. Adv. Enzymol. Relat. Areas Mol. Biol. **47**, 45–148

45 Blaber, M., Zhang, X. J. and Matthews, B. W. (1993) Structural basis of amino acid α helix propensity. Science **260**, 1637–1640

Received 13 June 2003/16 December 2003; accepted 17 December 2003
Published as BJ Immediate Publication 17 December 2003, DOI 10.1042/BJ20030884